ISSN 1070-3632, Russian Journal of General Chemistry, 2014, Vol. 84, No. 5, pp. 1050–1057. © Pleiades Publishing, Ltd., 2014.
Original Russian Text © N.N. Veniaminov, A.V. Smirnov, A.V. Berezin, A.Yu. Tarasov, 2012, published in Rossiiskii Khimicheskii Zhurnal, 2012, Vol. 56, Nos. 5–6, pp. 87–95.

Mass Spectrometric Determination of Uranium and Thorium Traces in Aerosols, Collected over Russian Territory after "Fukushima-1" Accident

N. N. Veniaminov[a], **A. V. Smirnov**[b], **A. V. Berezin**[b], **and A. Yu. Tarasov**[b]

[a] *Federal State Institution "12 CNII," Russian Ministry of Defense, Sergiev Posad-7, 141307 Russia*
[b] *Special Control Service, Russian Ministry of Defense, ul. Rubtsovsko-Dvortsovaya 2, Moscow, 107014 Russia*

Received November 1, 2012

Abstract—Secondary Ion Mass-Spectrometry was used to detect the isotopes ^{238}U and ^{232}Th in aerosols, sampled after damage of the "Fukusima-1" atomic station. The isotopes present only on the surface of the particles, so, fuel assemblages were melted, and they penetrated into environment through the gaseous phase without leakage of a solid substance in the form of primary aerosols. The presence of ^{232}Th is treated as a sign of ^{233}U production.

DOI: 10.1134/S1070363214050429

INTRODUCTION

For the Comprehensive Nuclear Test-Ban the International Monitoring System is launched using four control methods: seismic, radionuclide, hydroacoustic and infrasound. On Russian territory monitoring stations operate under the auspices of Special Control Service of the Russian Ministry of Defense [1]. The Service includes the Central Laboratory of Radiation Control. In Russia, radionuclide control stations operate in Kirov, Norilsk, Peleduy, Bilibino, Ussuriysk, Zalesovo, Petropavlovsk-Kamchatsky and Dubna.

Technically, air radiation control includes collecting of aerosol samples using special filter material, briquetting and analysis of the briquettes by high-resolution gamma spectrometry directly at the station for the determination of volatile and short-lived radionuclides. Application of this method is regulated by the Treaty. The method does not require time-consuming sample preparation and measurements are simple, allowing quickly analyze samples on a daily basis. Performance of the filter system is known, so it is easy to calculate the absolute values of the isotope concentrations in the atmosphere. The results obtained are transferred to the official database of the International Monitoring System, while studied samples are deposited for storage in Vienna International Data Centre, where they can be requested by the countries participating in the agreement for more detailed study in national laboratories.

As for the analysis of samples collected over Russian territory, the staff of the Special Control Service use russian made APF type filters (Petryanov cellulose acetate filter) and analyze samples on the spot and in the central laboratory as witness samples. In the latter case, the samples are subjected to ashing in a muffle furnace at ~600°C to obtain compact specimens that can be analyzed by means of gamma end-detectors and using a more sensitive detector of "well" type. In this paper, the objects of study were bottom ash samples.

Problem and Solution

The earthquake and tsunami in northeastern Japan on March 11, 2011 led to a series of accidents at "Fukushima-1" nuclear power plant due to the failure of reactors' cooling systems, causing spewedge of radioactive products. During "standard," accounted by the project, accidents at nuclear power plants only gaseous fission products leak into environment, as well as nuclides having volatile precursors in the isobaric decay chains and formed from them directly into the atmosphere: isotopes of iodine, krypton, xenon and cesium, which is a daughter product of xenon. Emission of gases to the atmosphere happens not necessarily due to the massive destruction of the reactor, the gases may leave the active zone through microcracks in the reactor body. Later isotopes, except the noble gases, are adsorbed by atmospheric particles, which leads to the formation of secondary aerosols.

Weather conditions were such that over Russian territory radioactive products were first recorded in Petropavlovsk-Kamchatsky (peak activity occurred on 17–18 March 2011).

By means of high-resolution gamma spectrometry, in aerosol samples in addition to the isotopes ^{137}Cs, ^{131}I, ^{132}I, ^{133}I and ^{140}La were found not only fission products without volatile precursors in the isobaric decay chains [2], but also the products of neutron activation: ^{99m}Tc, ^{129}Te, ^{129m}Te, ^{132}Te, ^{136}Cs, ^{134}Cs, ^{110m}Ag, ^{24}Na. If the ratio of the activities of ^{134}Cs and ^{137}Cs is more than 0.01, it is concluded that the first isotope appeared not as a result of a nuclear explosion, when there is not enough time for its formation from ^{133}Cs, but has the "reactor" origin. In studied samples, this ratio reached ~0.7.

The presence in the samples of non-volatile products of nuclear reactions suggests that the fuel assemblies have melted and there was a leakage of some quantities of irradiated fuel (it is instructive that in the environment has got technetium formed by a chain consisting of only refractory elements: $^{99}\text{Zr} \rightarrow {}^{99}\text{Nb} \rightarrow {}^{99}\text{Mo} \rightarrow {}^{99m}\text{Tc}$). But whether the accident was accompanied by the release of solids or non-volatile products have got into the atmosphere through the gas phase via the leakage of volatile fission products? Theoretically it is quite possible: Zr melts at 1852°C, TeO_2 boils at ~1260°C, Na_2O at 1350°C, UO_2 vaporizes without decomposition at a temperature above 1400°C [3], etc. To answer this question it is necessary to experimentally determine the nature of the distribution of impurities in the aerosol particles. In the first case (solids release), they will be presented in the volume of the particles (primary particles) in the second case (product ejection with the gas phase), on the surface (secondary aerosols).

By means of bulk analysis method it is impossible to resolve this dilemma, for this purpose mass spectrometry of secondary ions, based on stratified sputtering of solid surface is ideal. Varying the rate of erosion one can study the elemental composition of layers on different depth, including analysis of outer monolayer. Isotope ^{238}U should undoubtedly serve as a tracer, which is a basis (by weight) of nuclear fuel from power reactors, in the melt its content is several orders of magnitude greater than any of above mentioned radionuclides [4, 5]. In case of the first scenario particles with high volume concentration of uranium should be found in the samples. Totally, more than two dozen of samples taken before and after the accident have been investigated.

In this paper we present the most spectacular results obtained for two samples collected on the territory of Petropavlovsk-Kamchatsky: sample 1 (collection date 17.03.11) and sample 2 (21.02.11).

EXPERIMENTAL

Investigations were carried out using a "Microlab" surface spectrometer, which was previously used to determine the isotopic composition of uranium particles for its model oxides [6], in the production dust particles of the nuclear fuel cycle plants[7] and in bulk samples of the armor-piercing projectile core material used by NATO forces in Yugoslavia. [8] The device is equipped with a gallium liquid metal gun (with ion energy up to 10 keV), argon gun (5 keV) and quadrupole mass spectrometer with proportional resolution across the mass scale from 1 to 800 AMU. Secondary ion detector is a secondary electron multiplier of channel type. A detailed description of technical capabilities of the instrument is given in [6, 9].

Installation scheme of "Microlab" and its operation principle is shown in Fig. 1. Analyzed surface is scanned by primary ion beam synchronously with the CRT beam, which brightness is modulated by secondary electrons flow ejected from the sample. As a result, the screen image of sprayed surface portion is formed. Raster size of primary ions can be discretely changed in accordance with the increase: 2×, 5×, 10×, etc. up to 500x, and the ion beam current can be varied in the range from nA fractions up to 150–200 nA for gallium gun and up to ~0.5 uA, for the argon one. Thus, it is possible to set the sample etching rate in a very broad range, including so-called static mode when only surface monolayer is eroded during experiment.

To produce preparations, particle suspension in acetone was applied dropwise onto the 10 mm graphite disk, glued with silver-containing composition to the standard sample mount of "Microlab" instrument. A binder was not added, the particles even without it kept well on the substrate surface after evaporation of acetone. The procedure was repeated until visually observed clusters of particles in the form of whitish spots had been formed on graphite surface.[1]

---

[1] Ash contains no organic substances, whose presence may lead to the charging of the surface by the ion beam, thus effectively draining the charge on the conductive substrate is guaranteed even if the particles are close to each other.

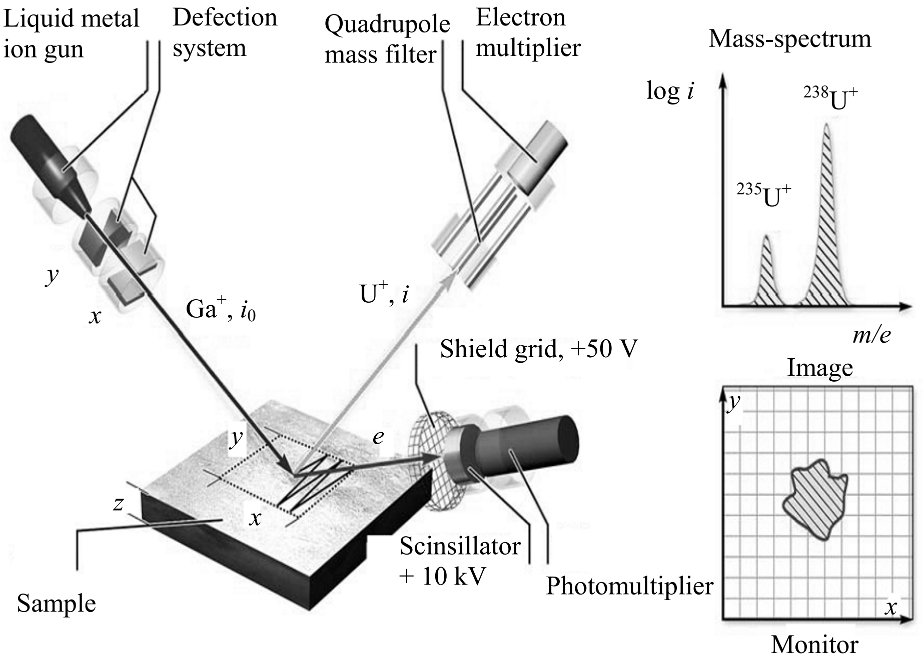

Fig. 1. "Microlab" instrument in ion microprobe mode.

To identify mounted on the substrate uranium containing micro objects a gallic liquid metal gun was used, providing high (~1 μm) lateral resolution, the mass spectrometer was set to max mass 254, and the output of the secondary ions UO^+ was controlled by the dial instrument with a scale ranging from 10 impulses/s up to 3×10^6 impulses/s. Primary ions current attributable to an individual particle is proportional to the share of the area occupied by it on the irradiated portion of the surface, so the smaller the raster, "covering" a particle, the higher the count rate of the secondary ions. Moving raster over the surface and sequentially compressing it, one can precisely locate the site where the object under study is, while it may not be seen on the screen, if it is too small. Once the particle is located, its targeted eroding is done, and at this time in fast mode (10sec per scan, in the range of 230-240 AMU) mass spectrum is recorded, which is used to calculate $^{235}U/^{238}U$ isotope ratio [7].

RESULTS AND DISCUSSION

Search for uranium particles in samples 1 and 2 using the procedure described above gave no results: on the substrate we were unable to locate such places, where the yield of secondary ions with a mass of 254 would be higher compared to neighboring areas, if any. Therefore, uranium particles, formed directly from the melt are absent in the sample 1. This conclusion is based on many years of experience in experimental analysis of samples taken from the territory of the nuclear fuel plants.

Positive result for sample 1 was achieved only if the surface layer was eroded with wide and intense beam of primary Ga^+ ions. This method can be regarded as an analogue to the gross analysis, not the total volume of the particles but of their surfaces composition. Figures 2 and 3 show the mass spectra obtained in those mass ranges where one can expect the emergence of secondary ions $^{238}U^+$ and $^{238}UO^+$ (above the peaks are their areas, expressed in counts). As can be seen, the identification of uranium and plutonium isotopes with odd mass impossible due to overlapping with emission clusters $BaGaO_2^+$, $Ga_3C_2^+$, $Na_5Cl_4^+$ [7], $BaGaO_3^+$ $Ga_3C_2O^+$ and $Na_4Cl_3Ca^+$, but for the even mass picture is different: for the 238th and 254th peaks a significant excess above the background is observed. A mass spectrum scan lasts 10 s, and the rate of sputtering is large enough (~0.1 nm/s). Therefore, in the course of the experiment the substrate under the influence of the ion beam was moved to capture new areas of its surface, not exposed to erosion, and thus simulate static mode dispersion (erosion within one monolayer). If not to do so, during recording of the mass spectrum elevation of uranium peaks above the background level becomes less noticeable, and then disappears. Conversely, the very

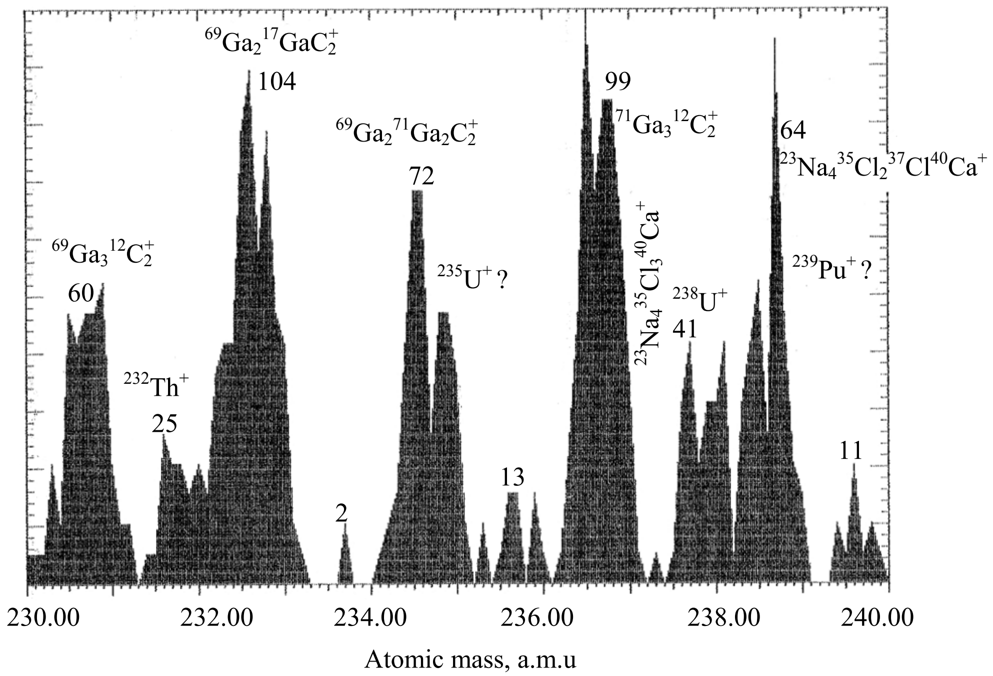

Fig. 2. Sample 1; Ga^+ primary ions with an energy of 8 keV; mass range 230–240. Ion beam current of 200 nA; raster area 0.55 mm^2; current density of 36 A/cm^2 on the sample; sputtering rate ~0.2 nm/s; 55 scans per mass spectrum, duration of a scan 10 s; sputtered layer thickness at a fixed raster ~110 nm.

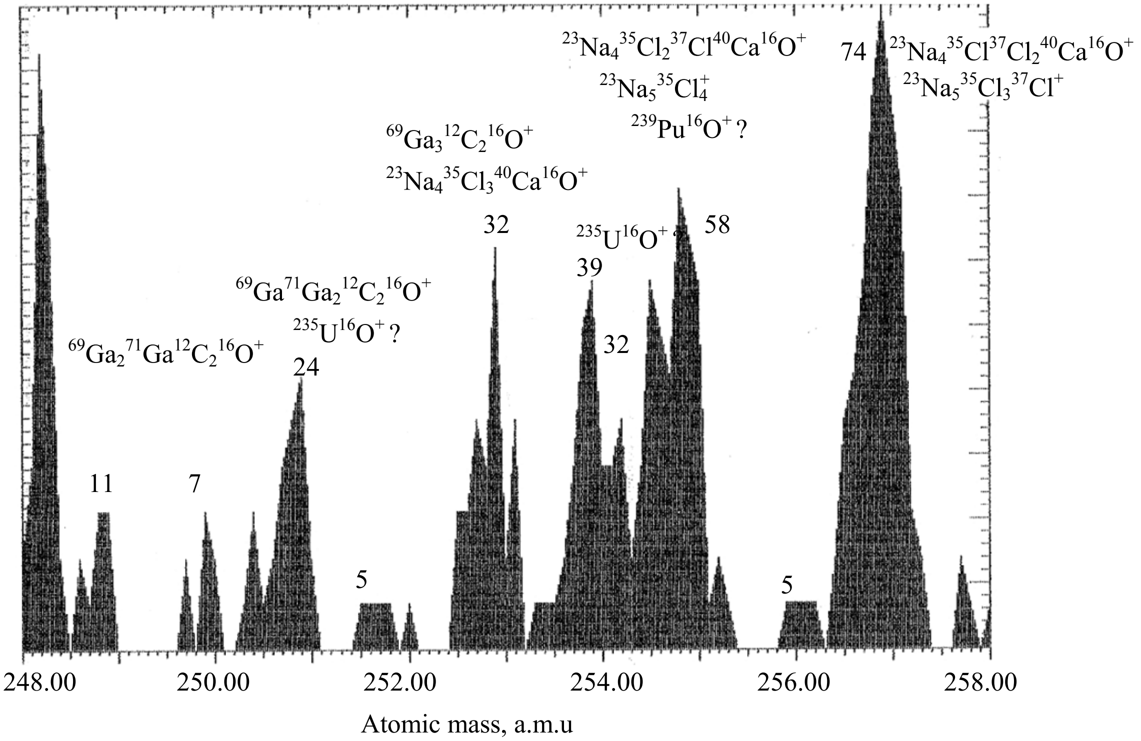

Fig. 3. Sample 1; Ga^+ primary ions with an energy of 8 keV; mass range 248–258. Ion beam current of 20 nA, raster area of 0.14 mm^2; current density of 14 A/cm^2 on the sample; sputtering rate ~0.08 nm/s; 31 scan per mass spectrum; sputtered layer thickness at a fixed raster ~25 nm.

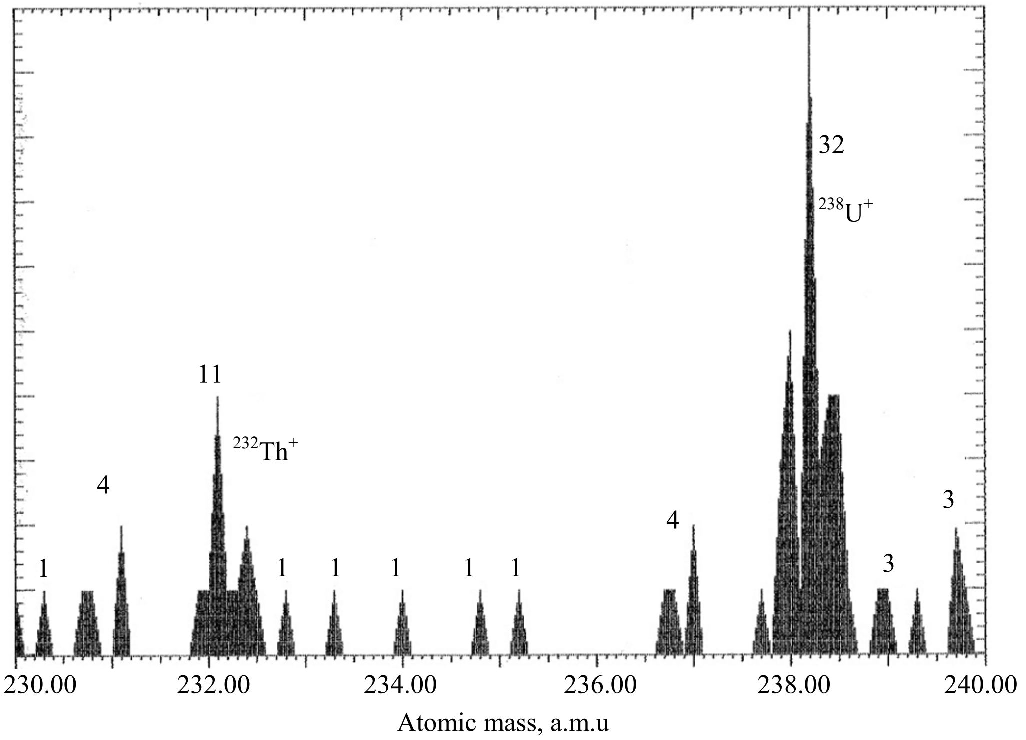

Fig. 4. Sample 1; Ar^+ primary ions with an energy of 5 keV; mass range 230–240. Ion beam current 410 nA; area of the irradiated surface $\pi/4$ cm^2; current density on the sample ~0.5 A/cm^2; sputtering rate ~10^{-3} nm/s; 17 scans per mass spectrum; the thickness of the sputtered layer ~0.2 nm.

first scan allows to register groups of pulses corresponding exactly to these masses and no others, the desired signal being reduced when recording even the second scan.

This means that the instrument does not "see" natural uranium distributed over the volume of the particles, due to the lack of sensitivity, and "sees" only those that "rests" on their surface and presented in larger concentrations, adsorbed reactor uranium. More convincing result was obtained when the entire surface of the graphite substrate with a diameter of 1 cm was subjected to the primary Ar^+ ion beam sputtering at ~10^{-3} nm/s rate (Figs. 4, 5). Galium containg complex ions were absent, and the peaks of $^{238}U^+$ and $^{238}U^{16}O^+$ were identified uniquely (for the comparison, Fig. 6 shows a mass spectrum of sample 2). Peak intensity ratio for 232 and 238 signals other than for the masses 248 and 254, consequently 232th isotope is not uranium. It is thorium, the same inverse ratio for outputs of secondary atomic and oxide ions of these elements was observed in [8], when using secondary ions spectrometry thorium coating not identified in the gross chemical analysis was discovered on the surface of depleted uranium core.

The uranium content in the sputtered layer was calculated according to the formula from [10]:

$$i_k = \mathrm{const}\cdot i_{ok}\cdot c_k\cdot \beta_k^+, \qquad (1)$$

where i_k is a singly charged positive ions counting rate; i_{ok} is a primary ion beam current in experiment to measure i_k; c_k is an atomic fraction of an isotope; β_k^+ is an ionization coefficient of the given element (the proportion of the sputtered atoms leaving the surface in the form of singly charged positive ions). Quantitative analysis by mass spectrometry of secondary ions is based on the use of standard samples. If the chemical state of an element is the same as in the test object, the matrix effects can be neglected and ionization coefficients considered to be constant. Knowing the concentration of an isotope in the standard sample c_m, the impurity concentration is calculated by the formula (2):

$$c_k = c_m[(i_k/i_{ok})/(i_m/i_{om})], \qquad (2)$$

where the expression in square brackets is the ratio of output of secondary ions per unit of the primary beam current in the test (numerator) and standard (denominator) samples.

As standard samples a strip of metallic uranium blackened on the air due to the formation on its surface

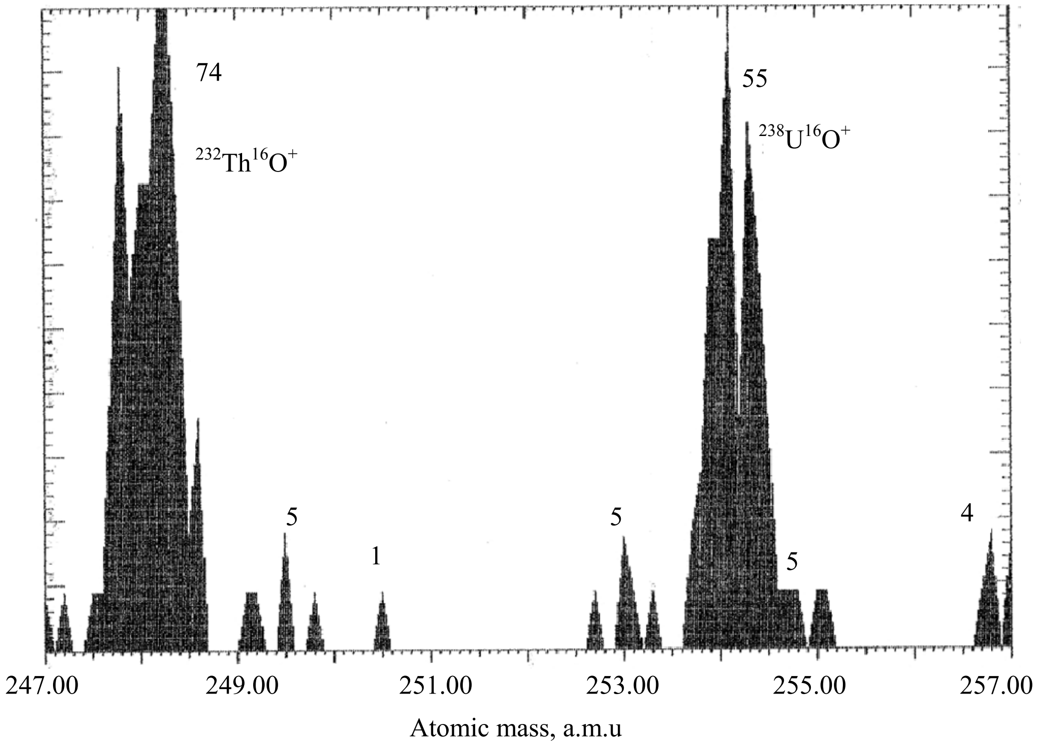

Fig. 5. Sample 1; Ar^+ primary ions with an energy of 5 keV; mass range 247–257. Ion beam current of 480 nA; area of the irradiated surface π/4 cm^2; the current density on the sample ~0.5 A/cm^2; sputtering rate ~10^{-3} nm/s; 30 scans per mass spectrum; the thickness of the sputtered layer ~0.3 nm.

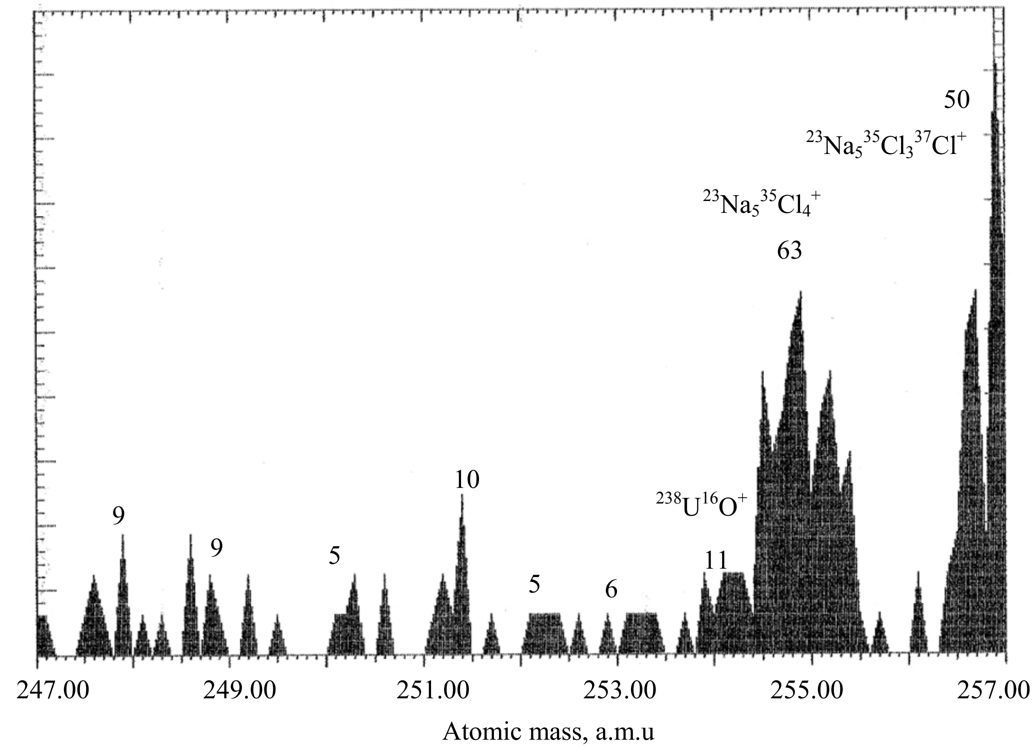

Fig. 6. Sample 2; Ar^+ primary ions with an energy of 5 keV; mass range 247–257. Ion beam current 410 nA; area of the irradiated surface π/4 cm^2; current density on the sample ~0.5 A/cm^2; sputtering rate ~10^{-3} nm/s; 31 scans per mass spectrum; the thickness of the sputtered layer ~0.3 nm.

UO_2 film[3,11], and silicon chip plate, film-coated with SiO_2 were used. For these samples under the same conditions from peak areas of $^{238}U^+$ and $^{28}Si^+$ relationships i_m/i_{om} were determined, which turned out to be, respectively, 10 ± 82 and 4560 ± 100 counts s^{-1} nA^{-1}. According to the formula (2) and the spectrum in Fig. 2 the average atomic fraction of uranium in the sprayed layer was calculated:

$c(^{238}\text{U}) = (1/3)\cdot 41/(55\cdot 200\cdot 82) = 1.5\times 10^{-5} = 15\pm 4$ ppm.[2]

According to the formula (2) and yield of secondary $^{28}Si^+$ions, equal to 3350 counts s^{-1} nA^{-1} (overview Mass Spectrum in 1-100 AMU range), Si concentration was calculated: $c(\text{Si}) = (1/3)(3350/4560) = 0.24 \pm 0.01$ (atomic fraction).

Below in descending order are listed 11 elements, that according to [3], compose more than 99% of Earth's crust mass, and the remaining are found at concentrations in order of hundredths of a wt % and less (uranium: 3×10^{-4} wt %). In parentheses are the atomic concentration calculated from the mass concentration and normalized to 1.

O (0.624), Si (0.208), Al (0.069), Fe (0.019), Ca (0.019),
Na (0.024), K (0.014), Mg (0.018), Ti (0.003), C (0.002),
Mn (0.0003), Th (7.3×10^{-7}), U (2.7×10^{-7})

These data show that silicon content in the sample is approximately the same as the average in the crust, while that of uranium in the sputtered surface layer, is 56 times greater. But that is not all: the measured concentration is the average of so many particles, most of which initially, priory to the manipulation with bottom ash were "clean." Hence, the particles related to the accident, "smeared" with reactor uranium even more thoroughly. At the same time, it is clear why little active isotope ^{238}U (decay constant $\lambda = \ln 2/T_{1/2} = 4.95 \times 10^{-18}\ s^{-1}$ [12]) was not detected using gamma spectrometry. Gamma-ray spectrometer does not "see" natural uranium and reactor uranium at a concentration sufficient for its detection, presented only in the surface layer of particles, which contribution to the total weight of the aerosol is too small (e.g., on the surface of a particle of 2 microns diameter with an atomic density of $5 \times 10^{22}\ cm^{-3}$ contains only 0.08% of the total number of atoms).

Thorium has a higher ionization potential (6.95 eV) than Uranium (6.08 eV), consequently, β^+_U/β^+_{Th} ratio must be greater than 1 since both impurities are in the same matrix. According to the model of local thermodynamic equilibrium [13] for the difference in ionization potentials of 0.87 eV and an effective electron temperature of 3000 K (kT = 0,26 eV) [9], the exponential terms in the Saha – Eggert equation for these two components differ by 28 times: exp(0.87/0.26) = 28. If one rely on this value, the concentrations of thorium and uranium, calculated by the mass spectrum (Fig. 2), will be related as 17 : 1. It turns out that the sample contains a few times more thorium, which oxide is exceptionally high melting (mp = 3200°C, bp = 4400°C [3]), than uranium (UO_2 vaporizes without decomposing at temperatures over 1400°C). This phenomenon can be explained by the fact that thorium was not part of the uranium fuel and was irradiated in the reactor separately to allow to extract by the chemical methods ^{233}U, which is formed from thorium:

$${}_{90}\text{Th}^{232}\,(n, \gamma) \rightarrow {}_{90}\text{Th}^{233}\,(\beta) \rightarrow {}_{91}\text{Pa}^{233}\,(\beta) \rightarrow {}_{92}\text{U}^{233}\ [3].$$

In the control of nuclear activities according to the analysis of finely dispersed products (one of the verification mechanisms of the Treaty on the Non-Proliferation of Nuclear Weapons [14]) method of mass spectrometry of secondary ions was successfully used for the isotopic analysis of individual micro-objects in a dynamic spraying mode [7, 15–19]. In this paper, another advantage of the method was fully manifested – the ability to analyze thin surface layers of the ensembles of particles in the spray mode, approaching the static mode. As such, the method of mass spectrometry of secondary ions was for the first time used for the diagnosis of the accident at the nuclear power plant [20], and this initiative has proved to be successful. We succeeded to independently establish that: (1) fuel elements have melted, (2) release of irradiated fuel in the solid state has not occurred, and (3) a small amount of it got into the environment through the gas phase via the leakage of volatile fission products. There are reasons to qualify used instrumental techniques based on mass spectrometry of secondary ions as a remote method of estimating state of the core and the reactor protection barriers after an accident.

REFERENCES

1. Vasilyev, A.P., Danilov, A.G., Donchenko, B.S., et al., *Dal'nevostochnyi debyut Sluzhby kontrolya yadernykh vzryvov* (Far East Debut of the Nuclear Explosions Control Service), Moscow: Polygraf Servis, 2010.

---

[2] Underestimated, since at such sputtering rate static mode as described above is not achieved.

2. Gusev, N.G., Rubtsov, P.M., Kovalenko, V.V., and Kolobashkin, V.M., *Radiatsionnye kharakteristiki produktov deleniya. Spravochnik* (Radiation Characteristics of Fission Products. Handbook), Moscow: Atomizdat, 1974, p. 28.
3. *Kratkaya khimicheskaya entsiklopediya* (Short Chemical Encyclopedia), vols. 1–5, Moscow: Sovetskaya Entsiklopediya, 1961, 1963, 1964, 1965, 1967.
4. *Advanced Fuel Cycle and Reactor Concepts. Report of INFCE Working Group 8*, Vien: IAEA, 1980.
5. Kolobashkin, V.M., Ruzhansky, P.A., Sidorenko, V.D., *Radiatsionnye kharakteristiki obluchennogo yadernogo topliva. Spravochnik* (Radiation Characteristics of Irradiated Nuclear Fuel. Handbook), Moscow: Energoatomizdat, 1983.
6. Veniaminov, N.N., Kolesnikov, O.N., and Stebelkov, V.A., *Zh. Analit. Khim*., 1991, vol. 46, no. 9, pp. 1776–1781.
7. Veniaminov, N.N., *Zh. Analit. Khim*, 2000, vol. 55, no. 3, pp. 294–301.
8. Veniaminov, N.N., Khovavko, S.A., Voronov, S.A., Orlov, S.L., Azarov, L.A., Arkhipov, S.Yu., and Evdokimov, T.N., *Zh. Analit. Khim*, 2003, vol. 58, no. 4, pp. 401–407.
9. Veniaminov, N.N., Balychenko, A.A., and Veniaminov, G., *Zh. Analit. Khim*, 1991, vol. 46, no. 9, pp. 1782–1786.
10. Werner, G., in *Electron and Ion Spectroscopy of Solids*, Firmens, L., Vennik, J., and Dekeyser, V., Eds., Moscow: Mir, 1981.
11. Katz, J. and Rabinovich, E., *Chemistry of Uranium*, Moscow, Izdatinlit, 1954, p. 142.
12. *Skhemy raspada radionuklidov. Energita i intensivnost' izlucheniya* (Radionuclides Decay Scheme. Energy and Intensity of the Radiation), ICRP Publication 38, part 2, vol. 2, Energoatomizdat, 1987.
13. Andersen, C.A. and Hinthorne, J.R., *Anal. Chem*., 1973, vol. 45, no 8, p. 1421.
14. Donohue, D.J., *Alloys and Compounds*, 1998, vols. 271–273, pp. 11–18.
15. Veniaminov, N.N., *Sb. Dokladov VIII Vserossiiskoi (mezhdunarod.) konferentsii "Fiziko-khimicheskie protsessy pri selektsii atomov i molekul"* [Proc. of the VIII All-Russian (Int.) Sci. Conf. "Physico-Chemical Processes in the Selection of Atoms and Molecules"], Moscow: CNIIatominform, 2003, pp. 251–256.
16. Veniaminov, N.N., *Aktual'nye problemy ekologii i prirodopol'zovaniya* (Actual Problems of Ecology and Environmental Management), issue 5, part 1, Moscow: Russian Peoples' Friendship University, 2003, pp. 41–57.
17. Veniaminov, N.N., *Vestn. Ross. Akad. Nauk*, 2004, vol. 74, no. 1, pp. 37–41.
18. Veniaminov, N.N., *Sb. Dokladov VIII Vserossiiskoi (mezhdunarod.) konferentsii "Fiziko-khimicheskie protsessy pri selektsii atomov i molekul"* [Proc. of the VIII All-Russian (Int.) Sci. Conf. "Physico-Chemical Processes in the Selection of Atoms and Molecules"], Moscow: CNIIatominform, 2004, pp. 162–165.
19. Veniaminov, N.N., *Ros. Khim. Zh*., 2007, vol. 51, no. 1, pp. 158–164.
20. Veniaminov, N.N., *Advanced Materials*, special issue no. 14, February 2013, pp. 123–127.